SUPPORTING INFORMATION

Fast Hydrazone Reactants: Electronic and Acid/Base Effects Strongly Influence Rate at Biological pH

Eric T. Kool*, Do-Hyoung Park, Pete Crisalli

Department of Chemistry, Stanford University, Stanford, CA 94305-5080 (USA)
*e-mail: kool@stanford.edu

Table of Contents

General. Compounds were obtained from Sigma-Aldrich except the following: 4-pyridine-carboxaldehyde, 4-chorobenzaldehyde, and terephthalaldehydic acid (TCI America), *d*-deoxyribose, acetophenone (Fluka), and 8-quinoline carboxaldehyde (VWR). Reaction buffer was prepared by mixing 10x phosphate-buffered saline solution pH 7.4 (Fisher Scientific) with deionized water and HPLC grade dimethylformamide (DMF, Fisher Scientific) in 1:9:1 ratio (vol:vol:vol) except where DMF was replaced by water as noted below (Table S2). Reactants were dissolved in spectrophotometric grade dimethylformamide (Fisher Scientific) immediately prior to reaction. Reactions were monitored on a Cary 100 Bio UV-Visible Spectrophotometer.

Kinetics methods. Reactions were performed under pseudo-first-order conditions in quartz cuvettes (5 mm path length; total volume ~700 μL) with solutions pre-equilibrated at room temperature (23 °C). 596 μL reaction buffer was pipetted into the cuvette, followed by 2.0 μL of a 300 mM aldehyde stock solution in spectrophotometric grade DMF. The solution was mixed by rapid pipetting up and down (170 μL volume) 25 times. A background spectrum was measured and stored. The reaction was then initiated by addition of 2.0 μL of 60 mM hydrazine stock solution with mixing by rapid pipetting up and down 25 times. The cuvettes were capped and spectra were measured repeatedly at 10 min intervals over 2-4 hours.

Faster reactions required 2x, 4x, and 8x dilution of the aldehyde and hydrazine stock solutions to slow reaction so that fitting could be performed adequately. The fastest reactions were measured every 5 min rather than the standard 10 min. Representative spectra (with background subtracted) as a function of time are shown in Fig. S1. For each pair of reactants we chose the wavelength of maximal change to follow time vs. absorbance data. Representative plots of these curves are shown in Fig. S2.

Fitting of the pseudo-first-order kinetics data was done by linear least-squares fits, following the Guggenheim (time lag) method.[1,2] In this method (see method II in ref. 2), the data obtained at regular intervals τ are divided into halves, and early absorbance data are substracted from the second-half data as shown in the following equation:

$$\ln(A_{t+\tau} - A_t) = \ln((A_{inf} - A_0)(1-e^{-k\tau})) - kt$$

This method removes the need for measuring a zero-time absorbance value and a final (infinity) absorbance value. The natural log of absorbance differences are plotted vs. time, and the slope corresponds to the negative of the pseudo-first-order rate constant. Representative linear fits are shown in Fig. S3. The first-order rate constants were obtained from the slopes of the linear fits, and were adjusted for units of seconds. Experiments were repeated 3-6 times and averaged, and standard deviations were obtained.

To serve as a check on rate constants obtained above, we also used the half-life method to estimate rate constants. In this method, we measured the time to reach 50% of the absorbance change ($t_{(1/2)}$) and then obtained the pseudo-first-order rate constant (k_{ps}) from the equation

$$t_{(1/2)} = 0.693/k_{ps}$$

The second-order rate constants were obtained from k_{ps}. and the reactant concentration. Very good agreement was seen with our reported rate constants (Tables 1,2 in main text).

Additional notes on kinetics methods:

(a) *On the possibility of non-second-order behavior*. The mechanism and kinetic behavior for imine formation between hydrazines and carbonyl compounds depends on multiple factors, including carbonyl structure, hydrazine structure, reactant concentrations and pH. We have tested a wide range of carbonyl structures in this study, and thus it is likely that not all cases tested here would reflect true second-order behavior if the kinetic mechanism were investigated in detail. The reader is cautioned that the second-order rate constants listed here are apparent values, and were simply obtained by calculation from the observed first-order rates that we measured spectroscopically. The observed pseudo-first-order rates are more reliable since they were measured directly.

(b) *On the possibility of reaction reversal (hydrolysis of hydrazones).* We considered the possibility that the reverse reaction, if it occurred on fast timescales that are competitive with hydrazone formation, might affect measured rate constants. The main concern here would be cases in which reversal occurs rapidly, on a timescale of minutes. For the majority of substrates, this appears unlikely, since "standard" hydrazones (2-hydrazinylpyridine with 4-formylbenzamides as calculated by Dawson, Bioconj. Chem. 2008, 19, 2543–2548) at pH 7 in the absence of catalyst give a hydrolytic rate (k_{-1}) of approx 10^{-6} per second, for a half-life of 8 days. We only measured reactions for minutes to hours, and saw clear plateauing of data (as expected) for the large majority of cases, indicating reversal is slower than could be measured under our conditions. However, in re-running data during revision, we did observe for two rapidly-reacting electron-deficient ketones (trifluoroacetone and acetylpyridine) an initial rise in absorbance followed by a drop over late timepoints, which may indicate reversal at longer timescales. In those cases we measured rate constants at the early timepoints, where the hypothetical reverse rate was still low due to low product concentration.

To summarize, if the reversal reaction is slow relative to hydrazone formation, then measurement of forward rates will not be affected greatly. If reversal is very rapid relative to hydrazone formation, then no hydrazone formation would be measurable. The middle regime, where reversal occurs on the order of the rate of formation, may result in downward curvature at late time points if slightly slower than the forward rate (noted above); if slightly faster or equal to the forward rate, then no downward curvature would be seen. This last case would result in an underestimate of forward rates. It would also be reflected in non-second-order behavior, which is not consistent with the two measured cases in Fig. S4.

(c) *Considerations of hydration effects.* We considered the possibility that hydration of some substrates might affect reaction rates. Hydration equilibria generally lie to the side of the nonhydrated form except in relatively electron-poor aldehydes/ketones. In our series, trifluoroacetone and perhaps dimethoxyacetaldehyde are likely to exist significantly if not primarily in the hydrated form. For alkyl aldehydes the equilibrium position is ca. 1:1, while aryl aldehydes are largely unhydrated. Buschmann's study of hydration rates (and by inference from the equilibrium position, dehydration rates (*Ber. Bunsenges. Phys. Chem.* 1982, *86*, 129) shows that hydration occurs in 2-4 minutes and thus dehydration (for most compounds) in that time or less. A similar effect could be speculated for hemiacetals (the three sugars tested here), which we find not to react particularly slowly. In any case, the observed rates are not corrected or adjusted for any hydration effects. Our studies are aimed at developing practical reactions in aqueous buffers at biological pH.

Fig. S1. Representative time-dependent UV-vis spectral changes during hydrazone formation with phenylhydrazine at pH 7.4. Spectra were measured at 10 min time points as described above.

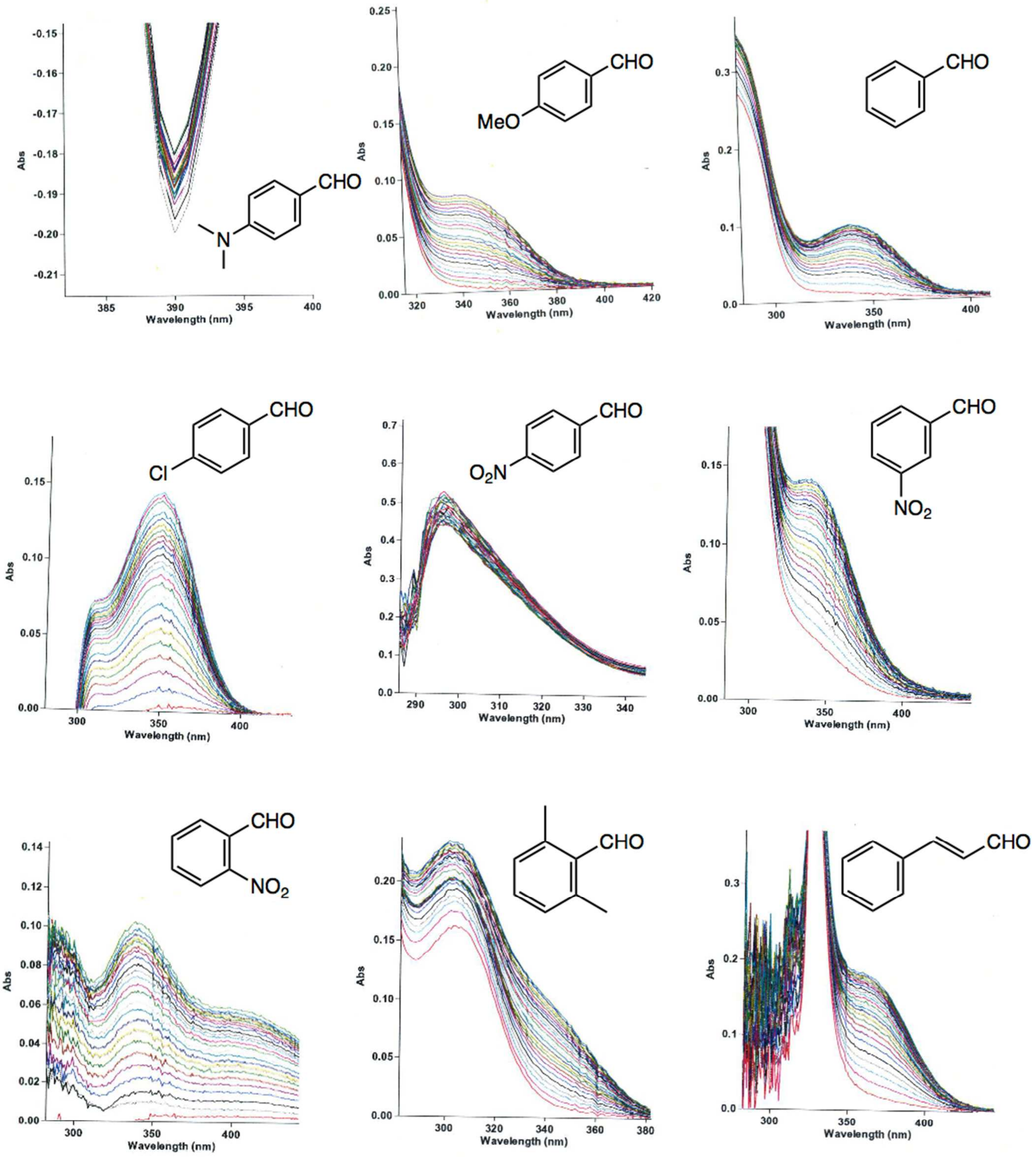

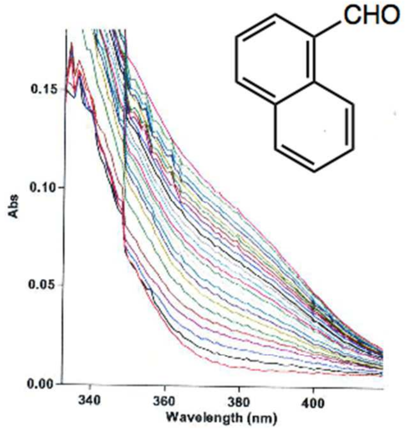
CHO
Abs
0.15
0.10
0.05
0.00
340
360
380
400
Wavelength (nm)

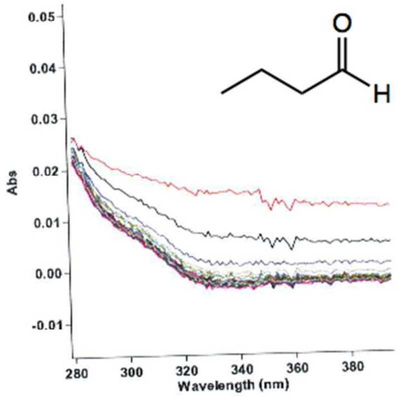
O
H
Abs
0.05
0.04
0.03
0.02
0.01
0.00
-0.01
280
300
320
340
360
380
Wavelength (nm)

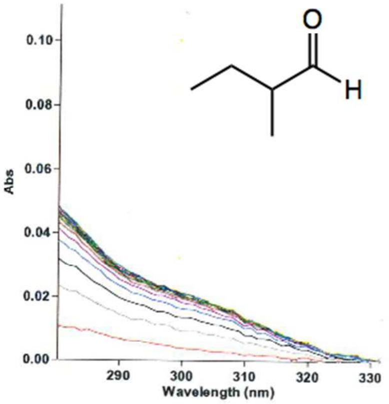
O
H
Abs
0.10
0.08
0.06
0.04
0.02
0.00
290
300
310
320
330
Wavelength (nm)

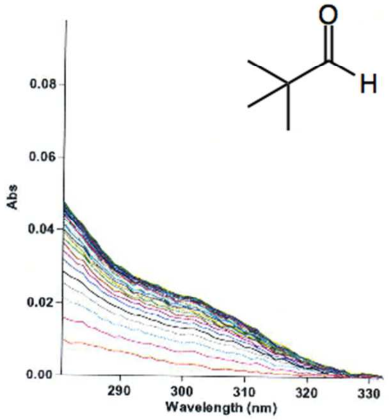
O
H
Abs
0.08
0.06
0.04
0.02
0.00
290
300
310
320
330
Wavelength (nm)

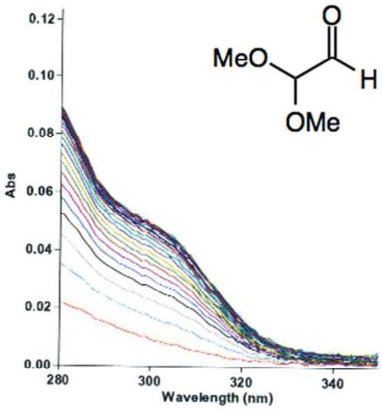
MeO
O
H
OMe
Abs
0.12
0.10
0.08
0.06
0.04
0.02
0.00
280
300
320
340
Wavelength (nm)

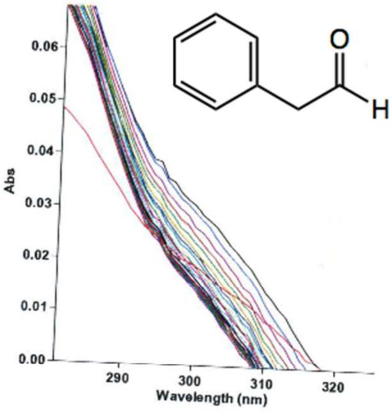
O
H
Abs
0.06
0.05
0.04
0.03
0.02
0.01
0.00
290
300
310
320
Wavelength (nm)

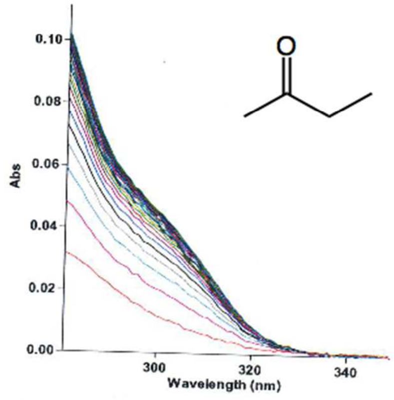
O
Abs
0.10
0.08
0.06
0.04
0.02
0.00
300
320
340
Wavelength (nm)

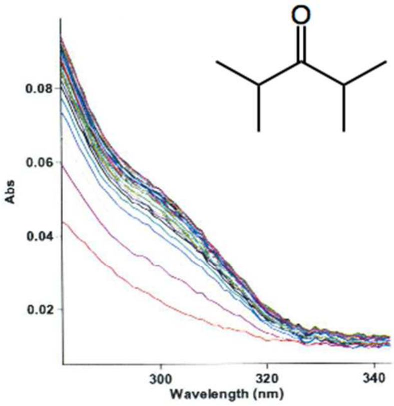
O
Abs
0.08
0.06
0.04
0.02
300
320
340
Wavelength (nm)

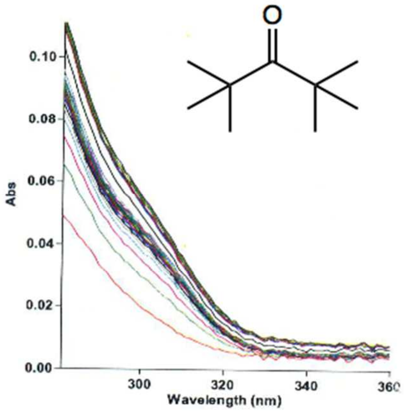
O
Abs
0.10
0.08
0.06
0.04
0.02
0.00
300
320
340
360
Wavelength (nm)

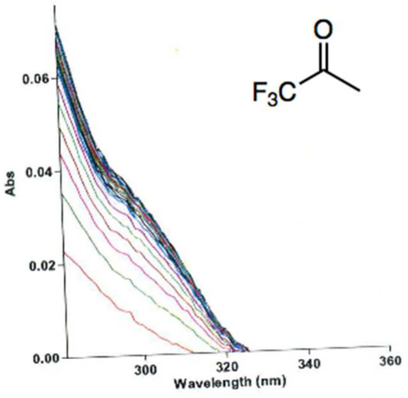

Abs
0.00
0.02
0.04
0.06
300
320
340
360
Wavelength (nm)
F3C
O

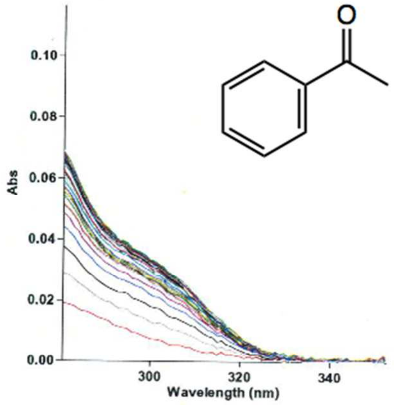

Abs
0.00
0.02
0.04
0.06
0.08
0.10
300
320
340
Wavelength (nm)
O

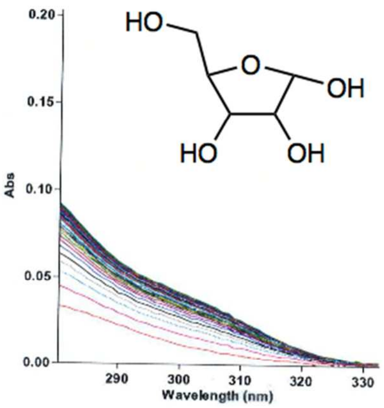

Abs
0.00
0.05
0.10
0.15
0.20
290
300
310
320
330
Wavelength (nm)
HO
O
OH
HO
OH

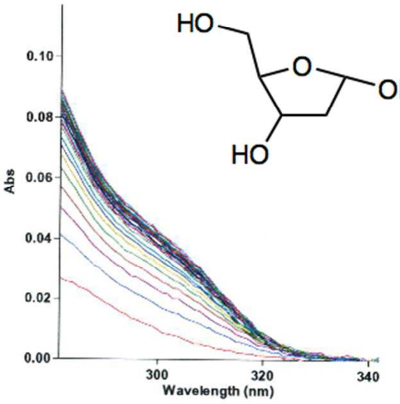

Abs
0.00
0.02
0.04
0.06
0.08
0.10
300
320
340
Wavelength (nm)
HO
O
OH
HO

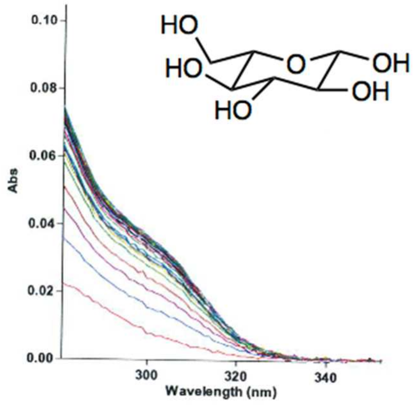

Abs
0.00
0.02
0.04
0.06
0.08
0.10
300
320
340
Wavelength (nm)
HO
HO
O
OH
OH
HO

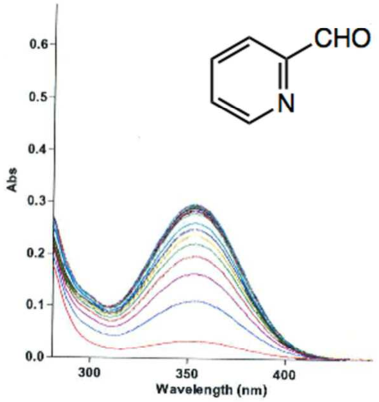

Abs
0.0
0.1
0.2
0.3
0.4
0.5
0.6
300
350
400
Wavelength (nm)
CHO
N

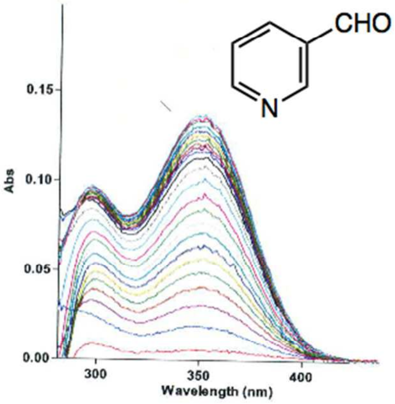

Abs
0.00
0.05
0.10
0.15
300
350
400
Wavelength (nm)
CHO
N

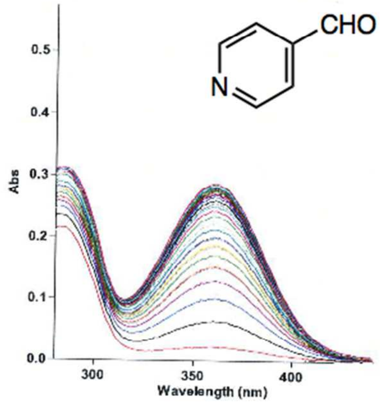

Abs
0.0
0.1
0.2
0.3
0.4
0.5
300
350
400
Wavelength (nm)
CHO
N

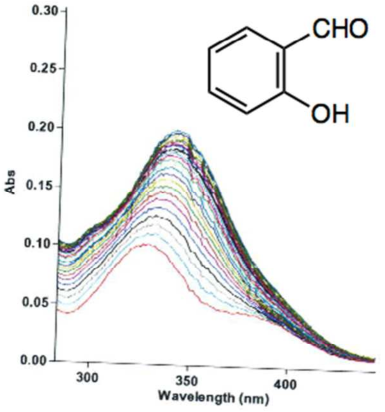

Abs
0.00
0.05
0.10
0.15
0.20
0.25
0.30
300
350
400
Wavelength (nm)
CHO
OH

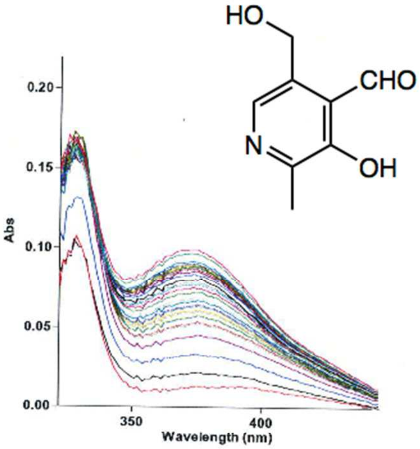
HO
CHO
N
OH
Abs
0.20
0.15
0.10
0.05
0.00
350
400
Wavelength (nm)

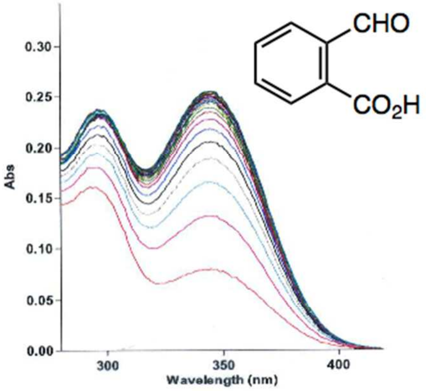
CHO
CO_2H
Abs
0.30
0.25
0.20
0.15
0.10
0.05
0.00
300
350
400
Wavelength (nm)

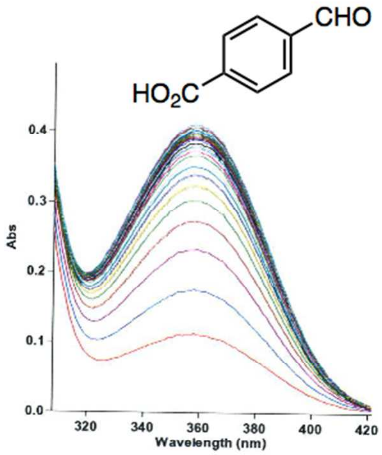
CHO
HO_2C
Abs
0.4
0.3
0.2
0.1
0.0
320
340
360
380
400
420
Wavelength (nm)

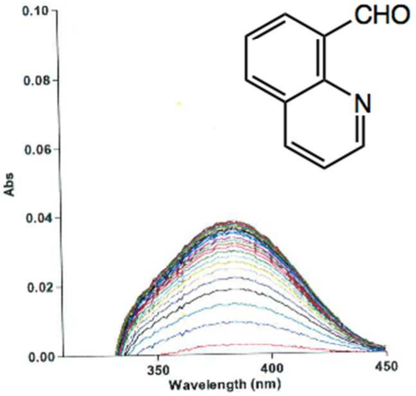
CHO
N
Abs
0.10
0.08
0.06
0.04
0.02
0.00
350
400
450
Wavelength (nm)

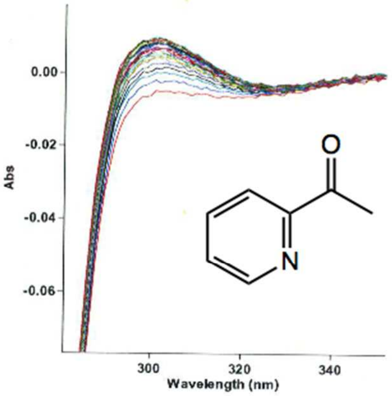
O
N
Abs
0.00
-0.02
-0.04
-0.06
300
320
340
Wavelength (nm)

Fig. S2. Representative plots of time-dependent absorbance changes during hydrazone formation of varied carbonyl compounds (shown) with phenylhydrazine at pH 7.4. Points were taken at 10 min intervals as described above.

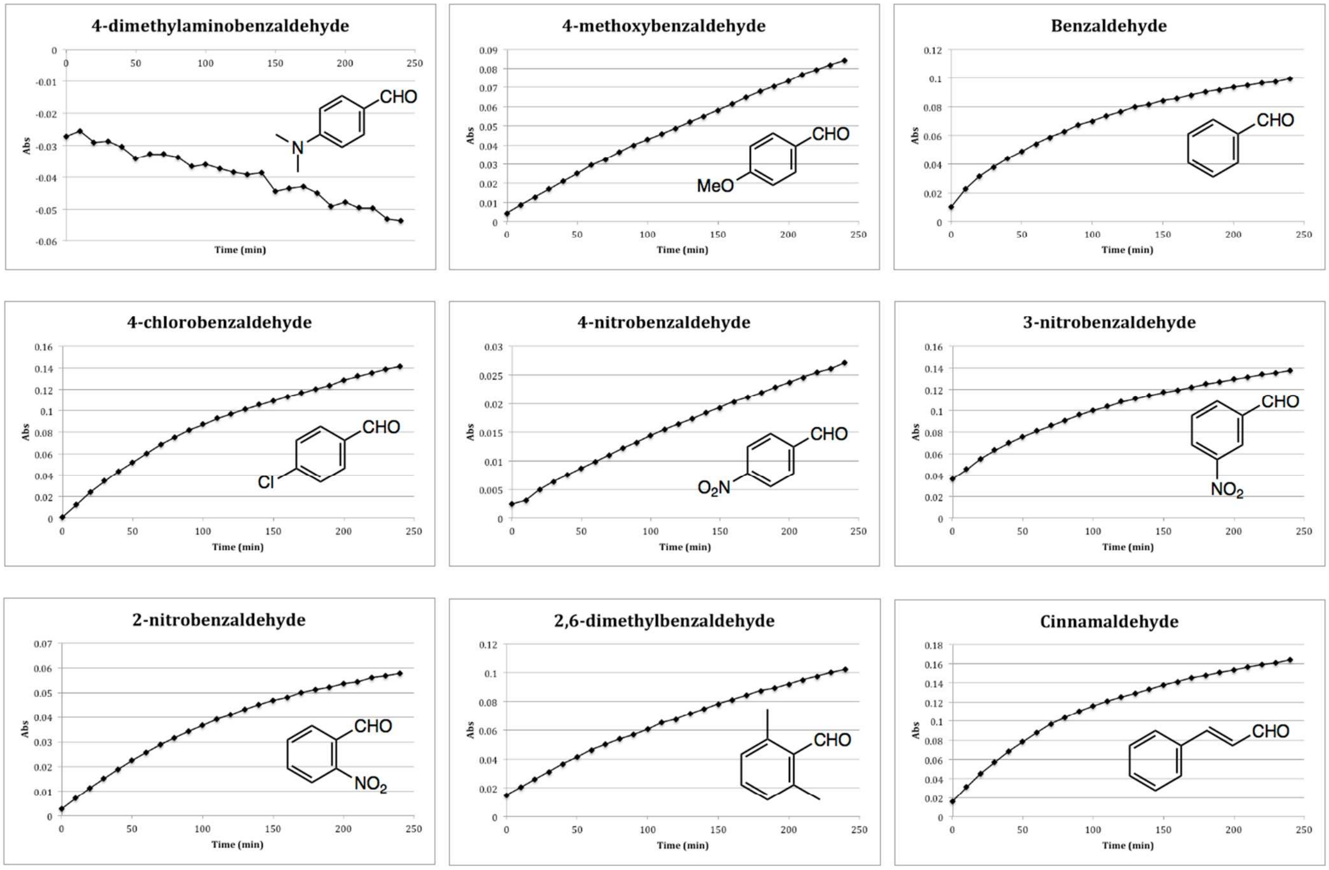

4-dimethylaminobenzaldehyde

4-methoxybenzaldehyde

Benzaldehyde

4-chlorobenzaldehyde

4-nitrobenzaldehyde

3-nitrobenzaldehyde

2-nitrobenzaldehyde

2,6-dimethylbenzaldehyde

Cinnamaldehyde

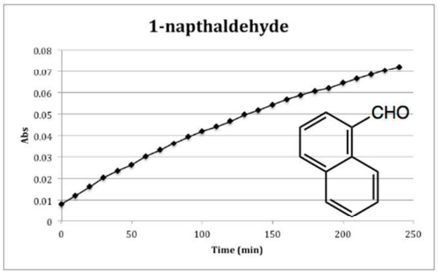
1-napthaldehyde
Abs
0.08
0.07
0.06
0.05
0.04
0.03
0.02
0.01
0
0
50
100
150
200
250
Time (min)
CHO

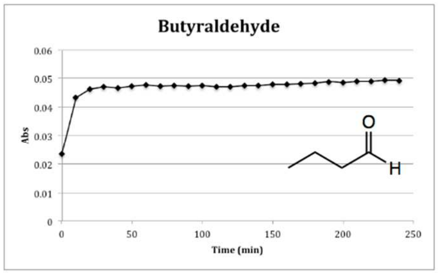
Butyraldehyde
Abs
0.06
0.05
0.04
0.03
0.02
0.01
0
0
50
100
150
200
250
Time (min)
O
H

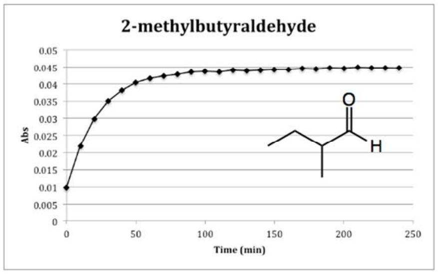
2-methylbutyraldehyde
Abs
0.05
0.045
0.04
0.035
0.03
0.025
0.02
0.015
0.01
0.005
0
0
50
100
150
200
250
Time (min)
O
H

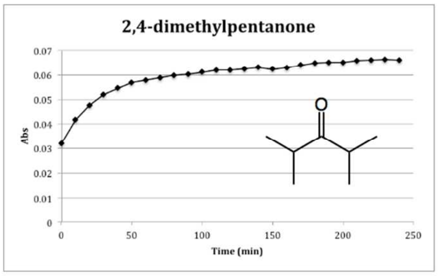
2,4-dimethylpentanone
Abs
0.07
0.06
0.05
0.04
0.03
0.02
0.01
0
0
50
100
150
200
250
Time (min)
O

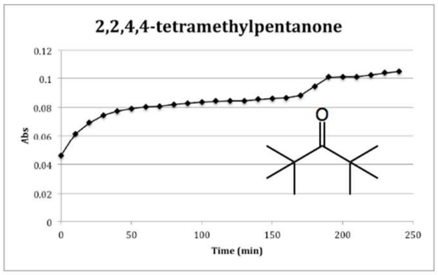
2,2,4,4-tetramethylpentanone
Abs
0.12
0.1
0.08
0.06
0.04
0.02
0
0
50
100
150
200
250
Time (min)
O

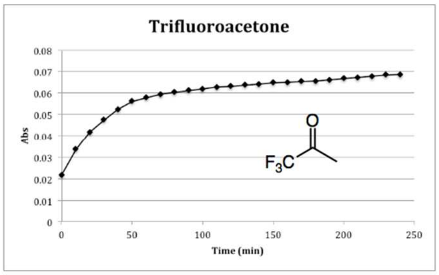
Trifluoroacetone
Abs
0.08
0.07
0.06
0.05
0.04
0.03
0.02
0.01
0
0
50
100
150
200
250
Time (min)
O
F3C

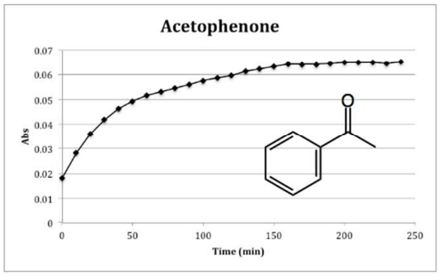
Acetophenone
Abs
0.07
0.06
0.05
0.04
0.03
0.02
0.01
0
0
50
100
150
200
250
Time (min)
O

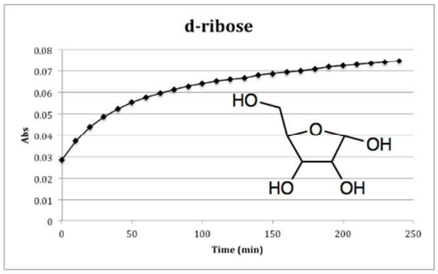
d-ribose
Abs
0.08
0.07
0.06
0.05
0.04
0.03
0.02
0.01
0
0
50
100
150
200
250
Time (min)
HO
O
OH
HO
OH

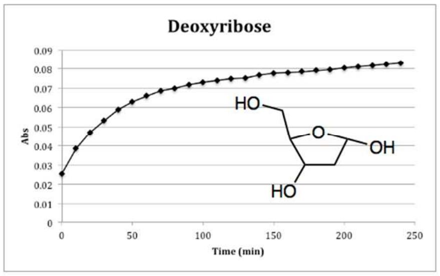
Deoxyribose
Abs
0.09
0.08
0.07
0.06
0.05
0.04
0.03
0.02
0.01
0
0
50
100
150
200
250
Time (min)
HO
O
OH
HO

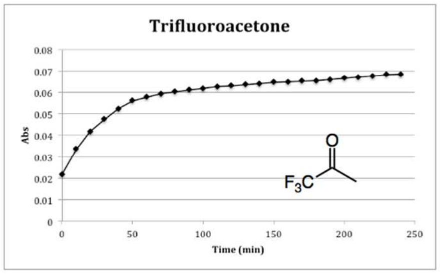

Trifluoroacetone

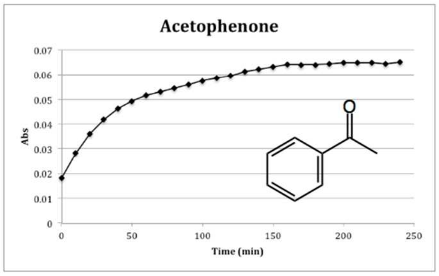

Acetophenone

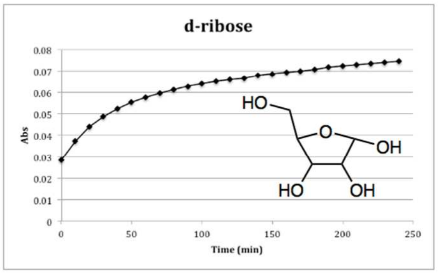

d-ribose

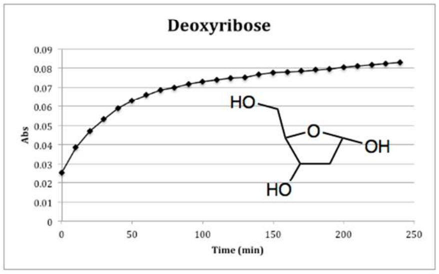

Deoxyribose

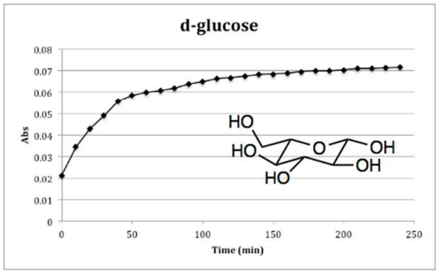

d-glucose

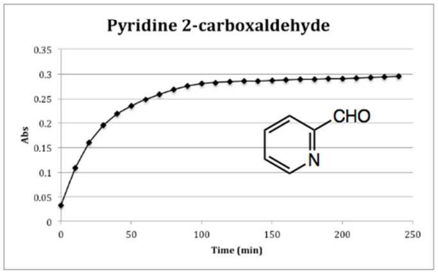

Pyridine 2-carboxaldehyde

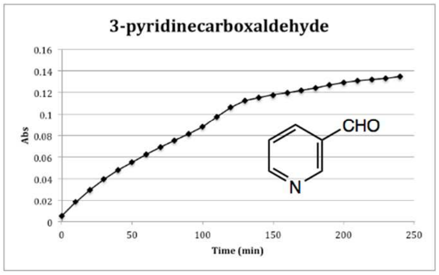

3-pyridinecarboxaldehyde

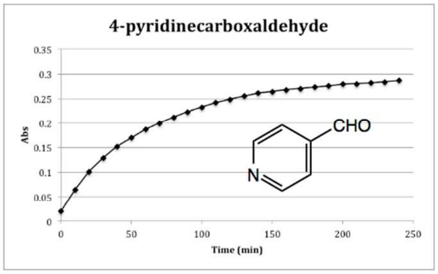

4-pyridinecarboxaldehyde

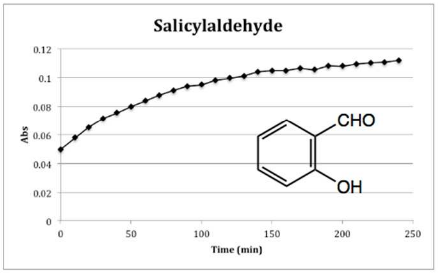

Salicylaldehyde

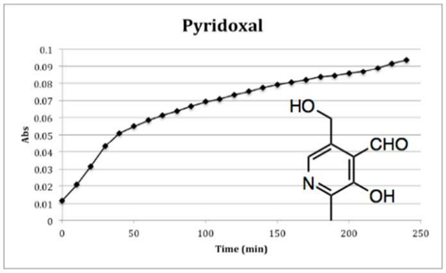

Pyridoxal

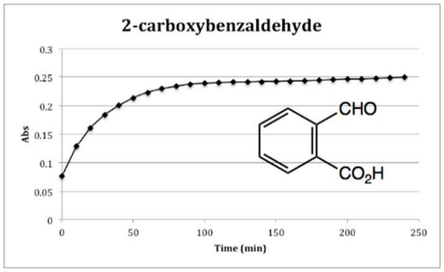

2-carboxybenzaldehyde

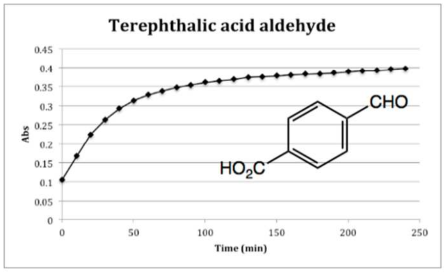

Terephthalic acid aldehyde

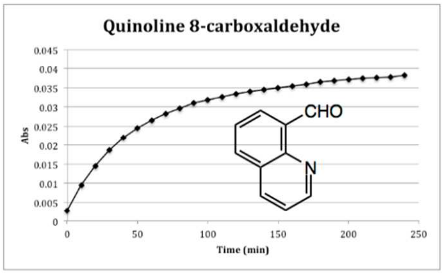

Quinoline 8-carboxaldehyde

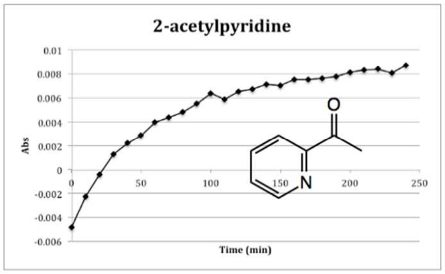

2-acetylpyridine

Fig. S3. Representative linear least-squares fits for hydrazone formation of compounds shown with phenylhydrazine at pH 7.4. Conditions were as described above. Fitting was done as described in ref. 2.

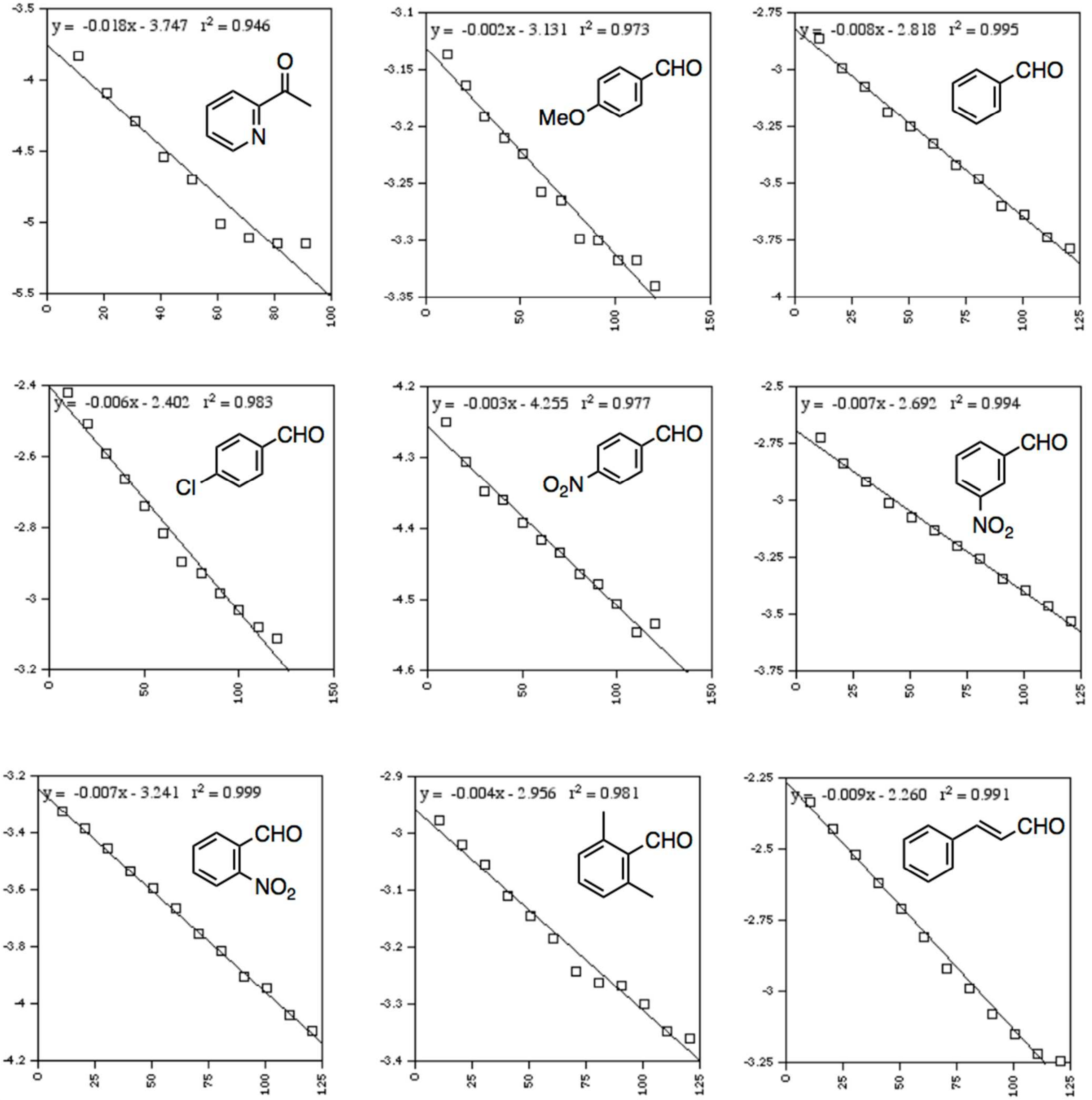

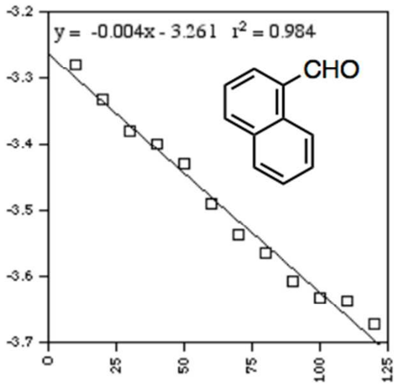
y = -0.004x - 3.261 r² = 0.984
CHO
-3.2
-3.3
-3.4
-3.5
-3.6
-3.7
0
25
50
75
100
125

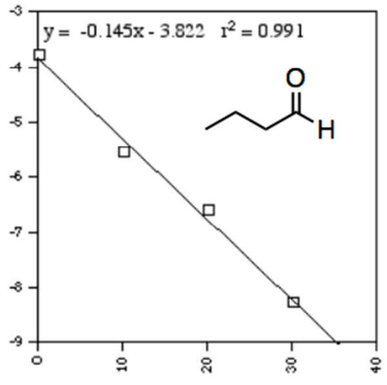
y = -0.145x - 3.822 r² = 0.991
O
H
-3
-4
-5
-6
-7
-8
-9
0
10
20
30
40

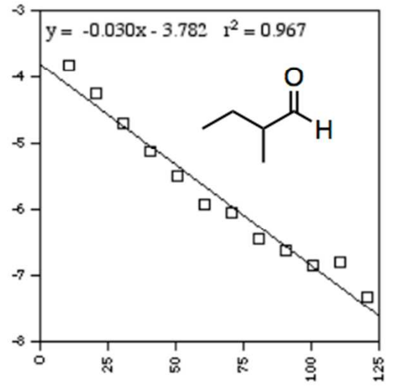
y = -0.030x - 3.782 r² = 0.967
O
H
-3
-4
-5
-6
-7
-8
0
25
50
75
100
125

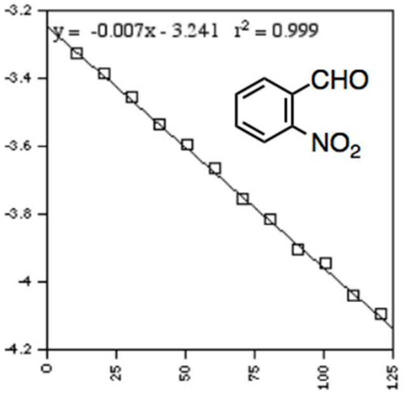
y = -0.007x - 3.241 r² = 0.999
CHO
NO₂
-3.2
-3.4
-3.6
-3.8
-4
-4.2
0
25
50
75
100
125

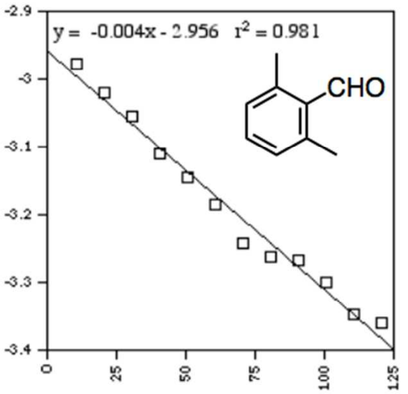
y = -0.004x - 2.956 r² = 0.981
CHO
-2.9
-3
-3.1
-3.2
-3.3
-3.4
0
25
50
75
100
125

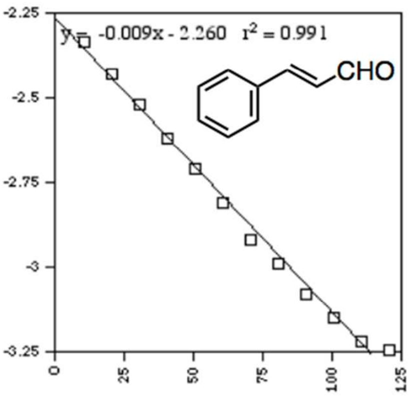
y = -0.009x - 2.260 r² = 0.991
CHO
-2.25
-2.5
-2.75
-3
-3.25
0
25
50
75
100
125

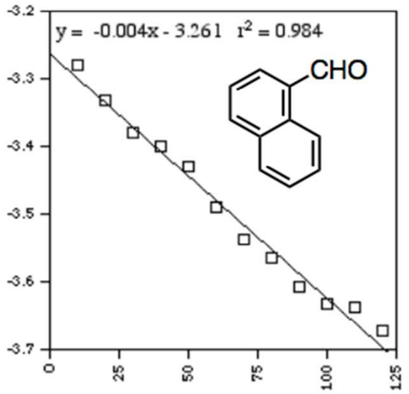
y = -0.004x - 3.261 r² = 0.984
CHO
-3.2
-3.3
-3.4
-3.5
-3.6
-3.7
0
25
50
75
100
125

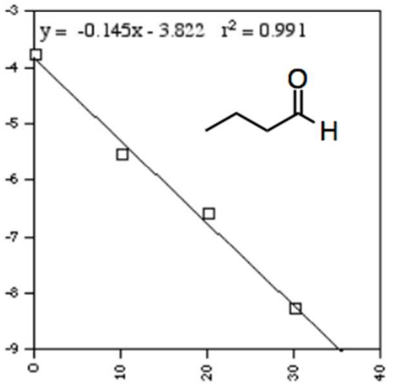
y = -0.145x - 3.822 r² = 0.991
O
H
-3
-4
-5
-6
-7
-8
-9
0
10
20
30
40

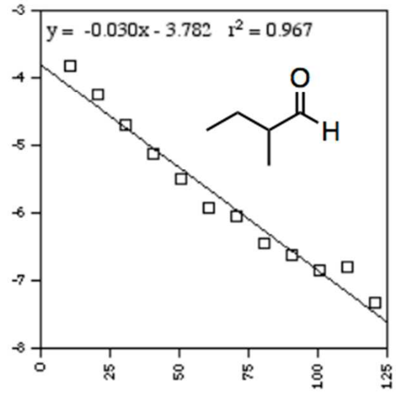
y = -0.030x - 3.782 r² = 0.967
O
H
-3
-4
-5
-6
-7
-8
0
25
50
75
100
125

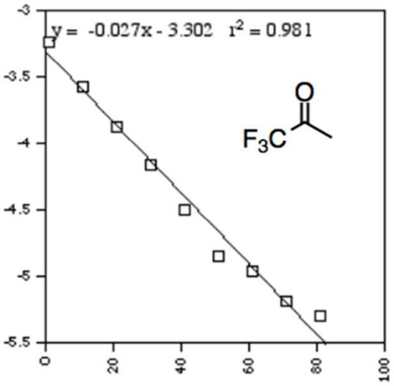
y = -0.027x - 3.302 r^2 = 0.981
O
F_3C
-3
-3.5
-4
-4.5
-5
-5.5
0
20
40
60
80
100

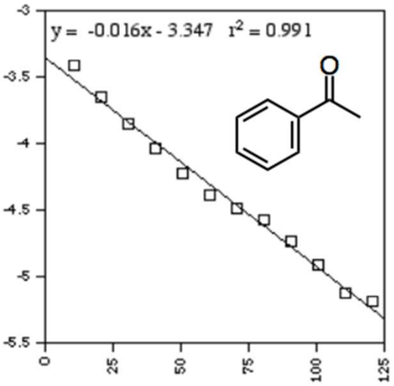
y = -0.016x - 3.347 r^2 = 0.991
O
-3
-3.5
-4
-4.5
-5
-5.5
0
25
50
75
100
125

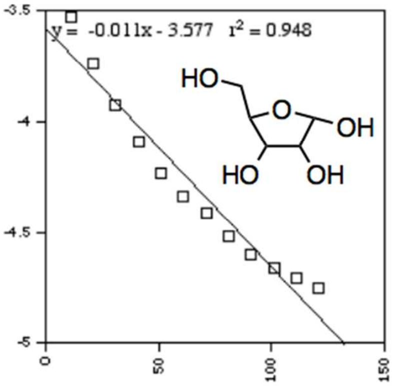
y = -0.011x - 3.577 r^2 = 0.948
HO
O
OH
HO
OH
-3.5
-4
-4.5
-5
0
50
100
150

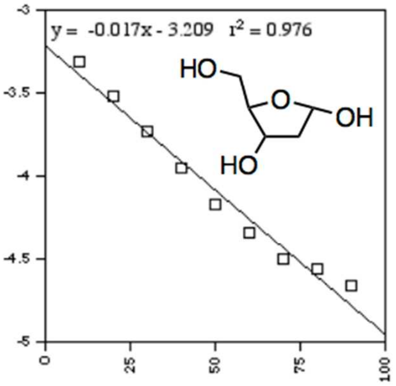
y = -0.017x - 3.209 r^2 = 0.976
HO
O
OH
HO
-3
-3.5
-4
-4.5
-5
0
25
50
75
100

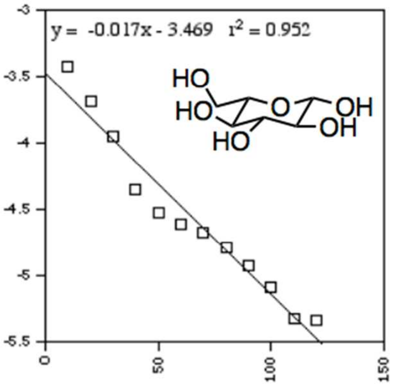
y = -0.017x - 3.469 r^2 = 0.952
HO
HO
O
OH
OH
HO
-3
-3.5
-4
-4.5
-5
-5.5
0
50
100
150

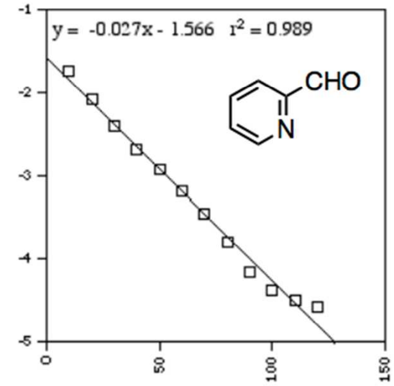
y = -0.027x - 1.566 r^2 = 0.989
CHO
N
-1
-2
-3
-4
-5
0
50
100
150

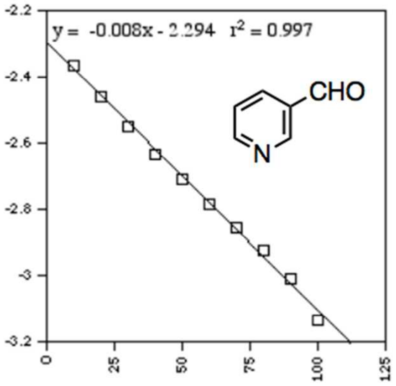
y = -0.008x - 2.294 r^2 = 0.997
CHO
N
-2.2
-2.4
-2.6
-2.8
-3
-3.2
0
25
50
75
100
125

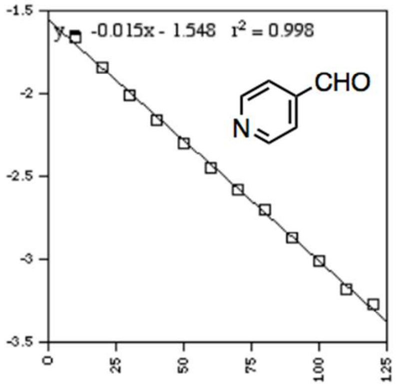
y = -0.015x - 1.548 r^2 = 0.998
CHO
N
-1.5
-2
-2.5
-3
-3.5
0
25
50
75
100
125

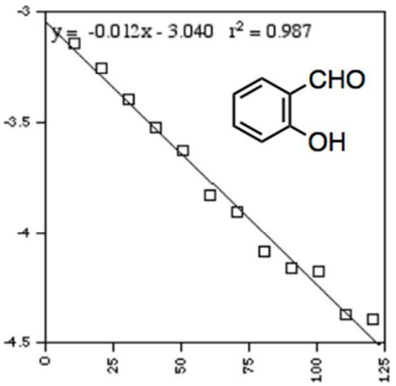
y = -0.012x - 3.040 r^2 = 0.987
CHO
OH
-3
-3.5
-4
-4.5
0
25
50
75
100
125

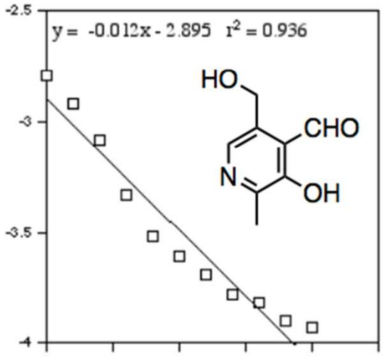
y = -0.012x - 2.895 r² = 0.936
HO
CHO
N
OH
-2.5
-3
-3.5
-4
0
25
50
75
100
125

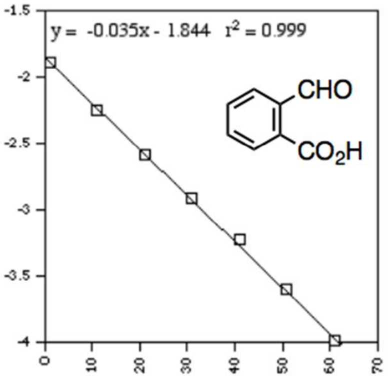
y = -0.035x - 1.844 r² = 0.999
CHO
CO₂H
-1.5
-2
-2.5
-3
-3.5
-4
0
10
20
30
40
50
60
70

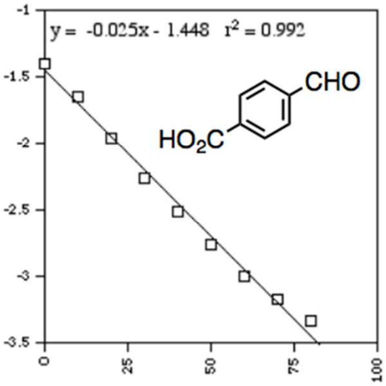
y = -0.025x - 1.448 r² = 0.992
CHO
HO₂C
-1
-1.5
-2
-2.5
-3
-3.5
0
25
50
75
100

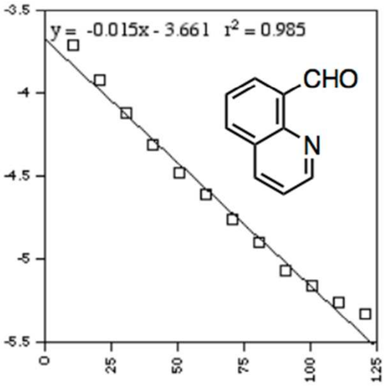
y = -0.015x - 3.661 r² = 0.985
CHO
N
-3.5
-4
-4.5
-5
-5.5
0
25
50
75
100
125

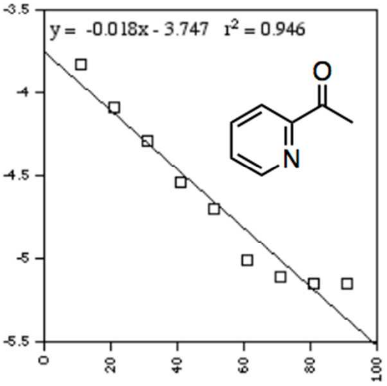
y = -0.018x - 3.747 r² = 0.946
O
N
-3.5
-4
-4.5
-5
-5.5
0
20
40
60
80
100

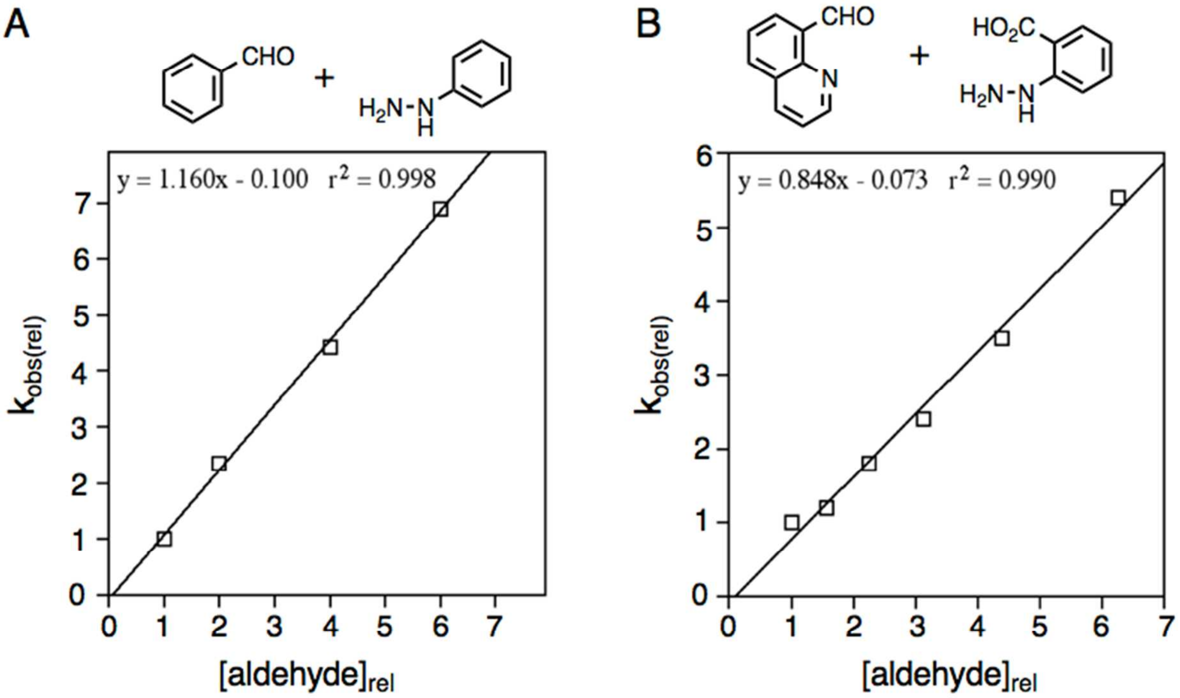

Fig. S4. Measuring kinetic order in aldehyde for two representative reactions. Shown are plots of relative observed pseudo-first-order reaction rates as a function of relative aldehyde concentration. Slopes denote kinetic order in aldehyde, which is ca. one in both cases. A. [aldehyde] range 200-1200 μM; [hydrazine] = 20 μM. B. [aldehyde] range 80-500 mM; [hydrazine] = 5 μM. Buffer is as per Table 1 legend.

Table S1. Long-wavelength absorption maxima of hydrazones in this study.[a]

hydrazone	λ_{max} (nm)	hydrazone	λ_{max} (nm)
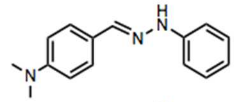	353	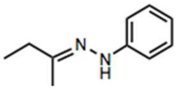	273
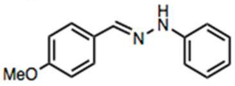	340	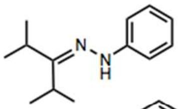	271
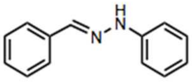	338	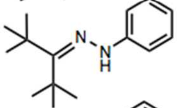	274
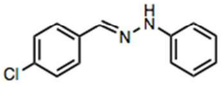	349	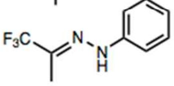	274
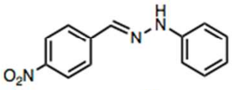	421	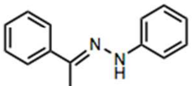	276
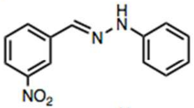	335	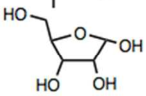	272
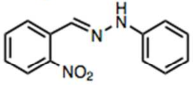	340	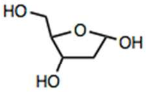	273
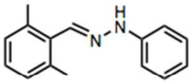	331	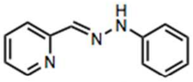	351
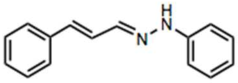	363	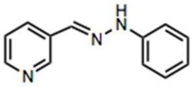	350
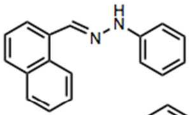	315	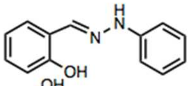	340
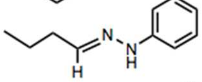	269	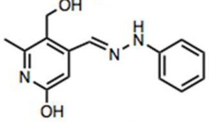	375
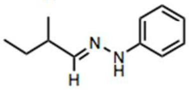	269	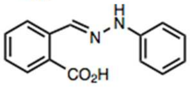	351
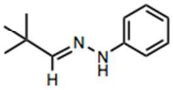	271	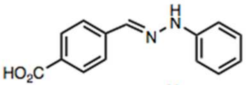	356
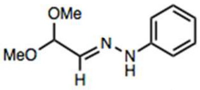	273	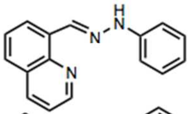	384
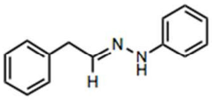	274	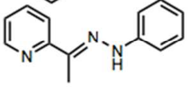	270

[a]Conditions: pH 7.4, 25°C, phosphate-buffered saline buffer with 10% DMF

Table S2. Effect of 10% DMF vs. Fully Aqueous Buffer on Selected Reaction Rates.[a]

reactants	buffer	$k_{1(obs)}$ (min^{-1})	$k_{2(app)}$ ($M^{-1}sec^{-1}$)	k_{rel}
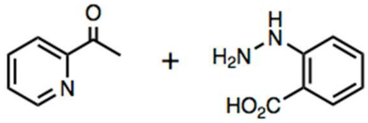	10% DMF	0.052 (0.005)	1.7 (0.2)	1
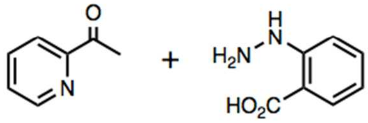	aqueous	0.016 (0.004)	0.55 (0.12)	0.3
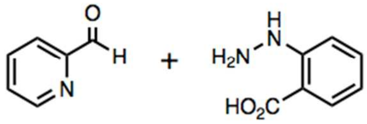	10% DMF	0.027 (0.002)	0.88 (0.05)	1
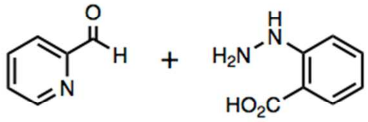	aqueous	0.023 (0.005)	0.77 (0.18)	0.9
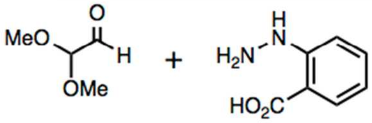	10% DMF	0.0070 (0.0002)	0.23 (0.01)	1
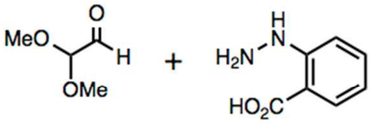	aqueous	0.0067 (0.0019)	0.22 (0.06)	1

[a] Conditions: pH 7.4, 25°C, phosphate-buffered saline buffer with or without 10% DMF. [Carbonyl compound] = 500 μM, [hydrazine] = 25 μM.

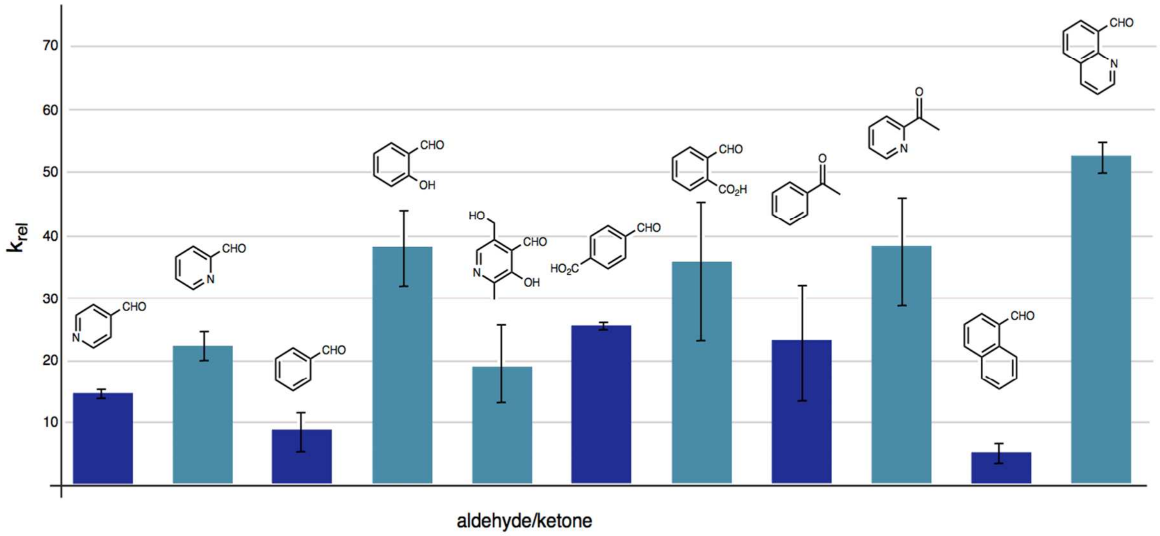

Fig. S5. Plot showing favorable effect of proximal acid/base groups on carbonyl compounds on rate of hydrazone formation with phenylhydrazine at pH 7.4. Conditions are as in Tables 1,2 (main text). Rates relative to 4-dimethylaminobenzaldehyde are shown. Dark blue = substrates with no proximal acid/base group; light blue = substrates with proximal groups.

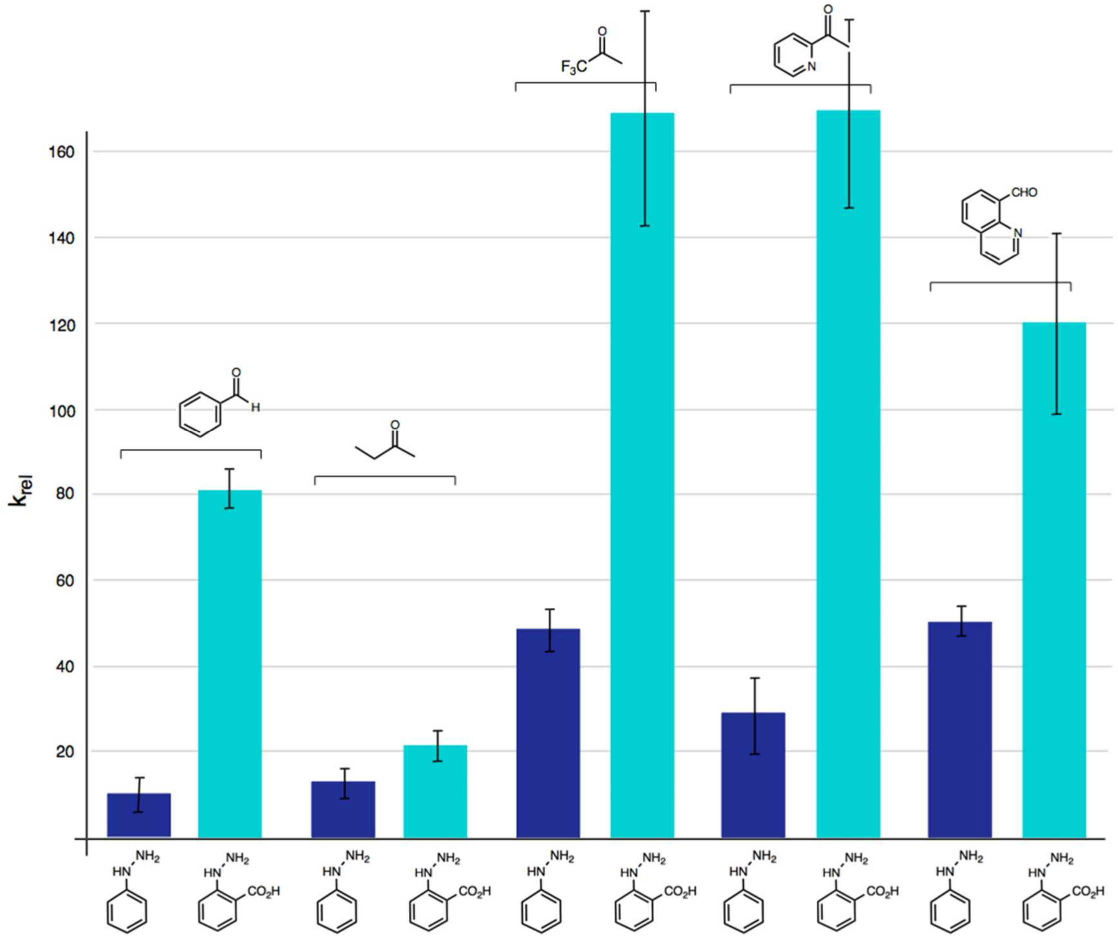

Fig. S6. Plot showing favorable effect of *ortho* carboxy group on the reactivity of phenylhydrazine with varied carbonyl compounds. Shown are rates of hydrazone formation at pH 7.4. Conditions are as in Tables 1,2 (main text). Rates relative to 4-dimethylaminobenzaldehyde are shown. Dark blue = phenylhydrazine reactions; light blue = *ortho*-carboxy-phenylhydrazine reactions.

References

1. Guggenheim, E. A. *Philos. Mag.* **1926**, *2*, 538.
2. Hemalatha, M. R. K.; NoorBatcha, I. *J. Chem. Ed.* **1997**, *74*, 972.